Long-circulating perfluorooctyl bromide nanocapsules for tumor imaging by 19FMRI

Odile Diou, Nicolas Tsapis, Céline Giraudeau, Julien Valette, Claire Gueutin, Fanchon Bourasset, Sandrine Zanna, Christine Vauthier, Elias Fattal

Long-circulating perfluorooctyl bromide nanocapsules for tumor imaging by ^{19}F-MRI

Odile Diou[1,2], Nicolas Tsapis[1,2], Céline Giraudeau[3], Julien Valette[3,4], Claire Gueutin[1,2], Fanchon Bourasset[5], Sandrine Zanna[6], Christine Vauthier[1,2], Elias Fattal[1,2]

[1] Univ Paris-Sud, UMR CNRS 8612, LabEx LERMIT, 5 rue Jean-Baptiste Clément, Châtenay-Malabry, France.

[2] CNRS, UMR 8612, 5 rue Jean-Baptiste Clément, Châtenay-Malabry, France.

[3] Commissariat à l'Energie Atomique (CEA), Institut d'Imagerie Biomédicale (I²BM), NeuroSpin, CEA Saclay, Bât. 145, F-91191, Gif-sur-Yvette cedex, France.

[4] Commissariat à l'Energie Atomique (CEA), Institut d'Imagerie Biomédicale (I²BM), Molecular Imaging Research Center (MIRCen), 18 route du panorama, BP n°6, F-92265, Fontenay-aux-Roses, France.

[5] Univ Paris-Sud, 5 rue Jean-Baptiste Clément, Châtenay-Malabry, France.

[6] Laboratoire de Physico Chimie des Surfaces, CNRS ENSCP (UMR 7045), Ecole Nationale Supérieure de Chimie de Paris (ENSCP), 11 rue Pierre et Marie Curie, Paris, France.

Introduction

From the 1970s, perfluorocarbons (PFCs) have been considered of great interest for clinical applications. They were initially developed as gas/oxygen carriers for lung ventilation or as blood substitutes [1-2]. Their high fluorine content, chemical inertness and variable physico-chemical properties, such as molecular weight, density or boiling point, widen their field of applications. Their potential as contrast agents is now well established as illustrated by their use in many different imaging modalities [3]. Mattrey and al. injected perfluorooctyl bromide (PFOB) in rabbits to detect liver-abscesses with Computed Tomography [4]. Perfluorohexyl bromide and PFOB helped to diagnose small-bowel obstruction during X-Ray examination [5]. Angiogenesis of breast cancer tumor was evidenced by ultrasonography with nanodroplets of perfluoropentane (T_b=28°C), which convert to highly echogenic nanobubbles upon heating to physiological temperatures [6]. Finally, Perfluoro-15-crown-5-ether (PFCE) emulsions were used for Magnetic Resonance Imaging either to label immunotherapeutic cells and follow their migration after administration or to visualize and quantify the development of neovasculature on atherosclerotic plaques [7-8].

The benefits of fluorine in MRI compared to proton-based imaging are numerous. ^{19}F has a spin ½ nucleus and a gyromagnetic ratio very close to the proton. Thus, for a given magnetic field value, the spin precesses at almost the same frequency, yielding a high sensitivity and allowing the use of proton spectrometer to detect fluorine. Moreover ^{19}F is found only in trace amounts in biological tissues, meaning that there is no endogenous background signal and that the signature of an exogenous fluorinated contrast agent is unique and specific. The choice of PFCs for ^{19}F MRI is crucial. PFOB is one of the most interesting because it is a FDA-approved dense liquid with a low diffusion coefficient into blood, increasing its residence time in the circulation as compared to other PFCs. Nevertheless, as observed for perfluorodecalin and perfluorohexane, PFOB has non equivalent fluorine nuclei, which induce a multi peak resonance spectrum leading to chemical shift artefacts with replicated images [9], and signal loss during echo time due to spin coupling. The recent design of a specific ^{19}F MRI multi spin echo (MSE) sequence allowed using PFOB as an MRI constrast agent while eliminating much of the restrictions associated with non-equivalent coupled nuclei [10].

Although most PFOB-based ^{19}F MRI contrast agents consist in emulsions [11-12], we have focused on recently developed polymeric nanocapsules of poly(lactide-co-glycolide) (PLGA), encapsulating PFOB [13-14]. The biodegradable polymeric shell ensures a good stability of the system, along with mechanical strength [15-16] as compared to emulsions. In addition, polymer chemistry offers versatility of chemical moieties, which can be further functionalized with targeted ligands [17] and

a loading compartment is made available in the shell for any lipophilic drug [18-19]. Preliminary *in vitro* ^{19}F MRI experiments revealed that encapsulation of PFOB within PLGA nanocapsules does not modify its contrast properties and may provide a significant contrast enhancement at 9.4T[14].

The *in vivo* use of PLGA/PFOB nanocapsules is however limited by their rather hydrophobic surface. After intravenous administration, PLGA nanocapsules undergo opsonization followed by rapid elimination by the mononuclear phagocyte system (MPS). Capsules end up mostly in the liver and the spleen and passive tumor targeting, based on the enhanced permeation and retention effect [20] cannot be achieved. To increase the plasmatic half life of nanocapsules, different strategies have been considered including surface modification of nanoparticles either with polysaccharides (dextran, heparin, chitosan) [21-22] or polyethylene glycol (PEG) chains [23]. The hydrophilic shell located on nanoparticle surface prevents opsonization by steric repulsion of blood proteins. PEG is FDA approved and PEGylation may be obtained by different methods such as physical adsorption, covalent grafting on preformed nanoparticles [24] or direct formulation using PEG-copolymers [25]. In the case of PLGA/PFOB capsules, decoration of the shell by PEGylated phospholipids was considered [3, 26-27] . This last strategy revealed deceitful. Since capsule mechanism of formation is exquisitely sensitive to interfacial phenomena [13] it was difficult to yield a good PEG coverage. The best PEG coverage obtained by this method expressed as the minimum surface occupied by one PEG chain, was 100nm². As PEG chains have a large range of motion, they may adopt a mushroom configuration or leave free spaces between each other allowing blood protein adsorption. In any case, the phospholipid strategy revealed unfavorable to reduce uptake by the MPS [3].

Our study focuses on the use of PLGA-PEG_{5000} diblock copolymer instead of PLGA to formulate PFOB nanocapsules. PFOB encapsulation within a polymer shell is exquisitely sensitive to the interfacial properties of both the polymer and the surfactant chosen, therefore requiring optimisation [13]. The encapsulation of PFOB will be optimized by comparing two formulation pathways: nanoprecipitation and emulsion-evaporation. The physico-chemical properties of the PEGylated nanocapsules will be assessed to validate their potential stealthiness after intravenous administration. Finally plain and PEGylated nanocapsules accumulation in liver, spleen and tumor will be measured by ^{19}F MRI to evidence the PEGylation efficacy.

Materials and methods

Materials

Methylene chloride (CH_2Cl_2) RPE-ACS 99.5% and Acetone 99.8% were provided by Carlo Erba Reactifs (France). Sulfuric Acid ACS Reagent 95-98% and $CDCl_3$ (99.96 atom % D) were provided by Sigma Aldrich (France). Poly(lactide-co-glycolide) Resomer RG502 (intrinsic viscosity 0.16-0.24 dl/g ; M_n=9 500-15 000 g/mol) and poly(ethylene glycol)-poly(DL-lactide-co-glycolide) 50:50 Resomer RGP d 50105 (intrinsic viscosity 0.72 dl/g ; PLGA M_n=45 000 g/mol containing 10 wt% of PEG M_n=5 000 g/mol) were obtained from Boehringer-Ingelheim (Germany). Poly(vinyl alcohol) (PVA) (M_W =30 000-70 000g/mol, 89% hydrolyzed) and sodium cholate (SC) were purchased from Sigma-Aldrich. Perfluorooctyl bromide (PFOB) and Perfluoro-15-crown-5-ether (PFCE) were purchased from Fluorochem (UK). Water was purified using a RIOS/Synergy system from Millipore (France).

Sample Preparation

Nanocapsules were prepared either by nanoprecipitation or emulsion-evaporation. In both cases, the polymer (100 mg) was dissolved into the organic phase along with 60 µL of PFOB and placed in a thermostated bath maintained at 20 °C. For nanoprecipitation, the aqueous phase (20 mL) was added quickly to the organic phase (acetone/CH_2Cl_2: 9.4 mL/0.6mL) with a syringe and needle, or opposite. For emulsion-evaporation, the organic phase (4 mL CH_2Cl_2) was emulsified into 20 mL of 1.5% sodium cholate (w/v) aqueous solution using a vortex for 1min and then a vibrating metallic tip (IBP7677, Ultrasons, Annemasse, France) at 180V, for 1 min over ice. Solvents were then evaporated by magnetic stirring at 300 rpm for about 3 h (for emulsion-evaporation) to overnight (for nanoprecipitation) in a thermostated bath (20 °C). Plain and PEGylated nanocapsules were prepared respectively with PLGA and PLGA-PEG copolymers. For plain nanocapsules, an incubation with PVA (1% w/v) for 5 days at 4°C is necessary, prior to the purification step, in order to replace sodium cholate by PVA and prevent further aggregation. Both types of nanocapsules were then washed by ultracentrifugation for 1 hour, at T=4°C and at 6 860 g, 27 440g for PLGA and PLGA-PEG nanocapsules respectively (Optima LE-80K Ultracentrifuge Beckman Coulter). The pellet was finally resuspended in water.

Size and Zeta potential

The hydrodynamic diameter (d_H) and polydispersity index (PDI) of the nanocapsules, were measured by quasi elastic light scattering, using a Zetasizer Nano ZS instrument (Malvern, France). Suspensions were diluted in water filtered over a 0.22 µm membrane. Measurements were performed in

triplicate at 20°C, at an angle of 173° to avoid multiple scattering. The counting time was set at 60s. Zeta potential measurements were carried out with the same instrument, at 25°C, in 1 mM NaCl.

Transmission Electron Microscopy (TEM)

Transmission electron microscopy was performed at CCME (Orsay, France) using a Philips EM208 operating at 80 kV. Suspensions of nanocapsules (1 mg/mL) were deposited on copper grids covered with a formwar film (400 mesh) for 2 min. The excess solution was blotted off using filter paper and grids were air dried before observation. Images were acquired using a high-resolution camera, Advantage HR3/ 12GO4 (AMT-Hamamatsu).

Scanning Electron Microscopy (SEM)

Scanning electron microscopy was performed using a LEO 1530 (LEO Electron Microscopy Inc, Thornwood, NY) operating between 1 and 3 kV with a filament current of about 0.5 mA. Washed and freeze dried nanocapsules were deposited on carbon conductive double-sided tape (Euromedex, France). They were coated with two palladium-platinum layers of ca. 1 nm using a Cressington sputter-coater 208HR with a rotary-planetary-tilt stage, equipped with an MTM-20 thickness controller. An In-lens detector has been used for imaging.

Determination of PFOB encapsulation efficacy by ^{19}F NMR

Fresh unpurified capsules were freeze dried for 24-48 h using an Alpha 1-2 LD plus freeze-dryer (Christ). Lyophilisates were then dissolved into $CDCl_3$ containing perfluoro-15-crown-5-ether (PFCE) as an internal standard ([PFCE]=0.76mmol/L). The amount of PFOB n_{PFOB}^{NMR} was determined after integration of the peak at -81ppm corresponding to the CF_3 group and normalization by the area of the PFCE peak at -89.5ppm. Encapsulation efficiency η_{encaps} was calculated as follows:

$$\eta_{encaps} = \frac{n_{PFOB}^{NMR}}{n_{PFOB}^{\max}} \text{ with } n_{PFOB}^{\max} = \frac{m_{PFOB}^{feed}}{M_{PFOB}} \frac{m_{NC}}{m_{PFOB}^{feed} + m_{Polymer}^{feed} + m_{SC}^{feed}}$$

where m_{PFOB}^{feed} $m_{Polymer}^{feed}$ m_{SC}^{feed} are the initial masses of the components introduced in the organic phase, m_{NC} corresponds to the mass of capsules recovered after freeze-drying and M_{PFOB} is the molecular weight of PFOB (498.96 g/mol).

Sodium cholate determination by spectrophotometry

The method used for sodium cholate assay was originally proposed by Mosbach and al. (1954) and then used by Dalwadi and al. [28-29]. Concentrated solutions were prepared by dissolving 25 to 125mg of sodium cholate up to 10mL of water. Aliquots of 40µL of each solution were pipetted

accurately into a 20mL volumetric flask, which is completed with freshly prepared 65% w/v sulfuric acid solution. Absorbance of the solution was measured at 320nm using a UV-Vis Spectrophotometer (Shimadzu UV-2101PC). Absorbance as a function of concentration of sodium cholate in sulfuric acid solution was plotted as a calibration curve over a concentration range from 5.0 to 25.0 µg/mL ($y=33.225x+0.0101$, $R^2=0.9999$).

A 25µL sample was taken from just-prepared nanocapsules suspension or supernatant of washed nanocapsules and placed into a 20mL volumetric flask. Final volume was completed with the 65% w/v sulfuric acid solution. Absorbance was measured at 320nm. The amount of sodium cholate was calculated using the calibration curve mentioned above. Experiment was done in triplicate for each sample.

To validate the accuracy of the method, a protocol derived from standard addition method, was used. Various volumes (from 5 to 13 µL) of suspension and 20 µL of the standard solution of sodium cholate ([SC]=5 µg/mL) were mixed into a 10 mL volumetric flask, completed with the 65% w/v sulfuric acid solution. Absorbance was plotted versus total concentration of sodium cholate ($y=33.021x+0.0087$, n=3 for PLGA and $y=34.508x+0.0144$ for PLGA-PEG). Assuming that only sodium cholate absorbs at 320 nm, the relative error on the attenuation coefficient is $\Delta\varepsilon/\varepsilon_0=0.61\%$ (with PLGA samples) and $\Delta\varepsilon/\varepsilon_0=3.86\%$ (with PLGA-PEG samples). It can be admitted that nanocapsules alone do not absorb at the considered wavelength.

Stability of nanocapsules over time

After purification, nanocapsules were dispersed in PBS and incubated at 37°C under stirring. Size variation of nanocapsules was followed with time by dynamic light scattering, as previously described. Simultaneously, aliquots of 2mL were taken out, freeze-dried and redispersed in $CDCl_3$. The volume of PFOB remaining encapsulated was evaluated by ^{19}F NMR.

X-ray Photoelectron Spectroscopy

X-ray photoelectron spectroscopy (XPS) was used to determine the surface composition of NPs. Powder of raw PLGA and PLGA-PEG polymers and lyophilisates of washed nanoparticles were deposited on the grid. A Thermo Electron Escalab 250 spectrometer with a monochromated radiation (1486.6 eV) was used. For all samples, a survey spectrum was recorded over a binding energy range of 0 to 1100 eV, the analyzer pass energy was 100 eV. In all cases the survey spectra only revealed the presence of oxygen (O1s 533 eV) and carbon (C1s 285 eV). C1s core was analysed in more details from 280 to 295 eV and pass energy of 20 eV. The spectrometer was calibrated against Au 4f7/2 at

84.1 eV. The photoelectron take-off angle (angle of the surface with the direction in which the photoelectrons are analyzed) was 90°. Curve fitting of the spectra was performed with the Thermo Electron Avantage software.

Complement Activation

The complement activation of PEGylated and non PEGylated nanocapsules was evidenced by evaluating the conversion of C3 into C3a and C3b by a 2-D immunoelectrophoresis method, as described by others [21, 30]. Human serum was obtained after calcifying plasma from healthy donors, and stored at -80 °C until use. Nanocapsule suspensions were incubated, under gentle agitation, for 1 h at 37°C with 50 µL human serum and 50 µL Veronal Buffer, containing 0.15mM calcium chloride and 0.5mM magnesium chloride (VBS^{2+}). To ensure a valid comparison of the different suspensions, concentrations in nanocapsules were adjusted to obtain an equal surface area of S =1000 cm^2 and 2000 cm^2 in 100µL. After incubation, 7 µL of each sample were subjected to a first electrophoresis on 1% agarose gel in tricine buffer (pH =8.6). The migration was achieved using Pharmacia LKR Multiphor (600 V, 8.8mA, and 5W) for 1.5 hours. The second-dimension electrophoresis was carried out for 18 hours, on Gelbond films in 1% agarose gel plates containing a polyclonal antibody to human C3 (Complement C3 antiserum rose in goat, Sigma, France), recognizing C3 as well as C3a and C3b. The films were finally dried and stained with Coomassie blue to reveal the presence of the proteins, which have reacted with the antibody (Sigma). The complement activation factor (CAF) was then calculated from the ratio of the total area of the peaks attributed to C3a and C3b over the sum of the areas of the peaks attributed to C3a+b and to C3. This ratio was then normalized on a scale ranging from 0 to 100 in which 100 indicated total activation, obtained with poly(isobutylcyanoacrylate) nanoparticles [31] and 0 the spontaneous activation, measured in absence of nanocapsules.

$$CAF = \frac{C3_{a+b}}{C3 + C3_{a+b}}$$

^{19}F MRI

In vivo accumulation study

Six-week-old females Foxn1nu (nu/nu) mice weighing from 20 to 22 g were purchased from Harlan (France). Animal procedures were in accordance with the recommendations of the EEC (86/609/CEE) and the French National Committee (decree 87/848) for the care and use of laboratory animals. Animals were anesthetized with ketamine and domitor. The ^{19}F Imaging was performed on a 7-T small-animal MRI scanner (Bruker, Ettlingen, Germany) using a double-tuned, ^{1}H/^{19}F 3.2-cm-diameter, linear, birdcage coil, built at Neurospin (CEA, Saclay, France). Anatomic ^{1}H images were

recorded at the beginning of the experiment to localize the organs. The multi spin echo imaging sequence (TE = 15.5 ms, TR = 4000 ms, 60 echoes one 16mm-thick slices, 0.63×0.94 mm^2 in-plane resolution) was used for ^{19}F imaging. It takes into account NMR properties of PFOB to maximize sensitivity [10]. Images were acquired every 4.5 minutes after intravenous infusion of the nanocapsules in the tail vein (200µL C_{PFOB}=120mM and 55mM respectively for plain and PEGylated nanocapsules). An external reference was placed close to the right flank of the mouse for signal calibration. Concentration of PFOB was measured as a function of time in the liver and spleen for 1.5 hours, multiplied by the volume of organs (V_{liver}=1mL and V_{spleen}=150µL) and normalised by the injected dose.

In vivo tumor imaging

Murine colon carcinoma cell line CT26.WT was purchased from ATCC (Molsheim, France). Four-week-old females Fox1nu (nu/nu) mice weighing around 20g were purchased from Harlan. The colon tumor model was established by injecting 3.10^5 cells (in 100 µL cell culture medium) subcutaneously into the right flank of the animal. Twelve days after tumor inoculation (V_{tumor}>150mm^3), PLGA and PLGA-PEG nanocapsules were injected in the tail vein (200µL, C_{PFOB}=82.5mM). 7 hours after the injection, the mouse was anesthetized with i.p. injection of ketamine and domitor and placed inside the coil. After acquisition of anatomical ^1H images, ^{19}F acquisitions were performed with the previously described MSE MRI sequence. Total acquisition time was 35min. Concentration of PFOB was measured in the liver, spleen and tumor multiplied by the volume of organs and normalised by the injected dose.

Results and Discussion

Formulation process

PLGA/PFOB nanocapsules were previously prepared by an emulsion-evaporation process which allowed modulating capsule diameter and thickness by simply varying the sonication power, the sodium cholate (SC) concentration or the PLGA/PFOB proportions [14, 32]. Another process has been fully reviewed in the literature to produce polymeric capsules: solvent displacement method, often called nanoprecipitation. Since it is a spontaneous process, the energy input is reduced. Besides, the use of surfactants may be optional and purification issues may be avoided. Considering these advantages and the amphiphilic nature of PLGA-PEG, nanoprecipitation was considered as an alternative to produce PLGA-PEG/PFOB nanocapsules. The mixture of acetone and methylene chloride (9.6mL/0.4mL) was chosen to ensure miscibility with water and full solubility of PFOB as well

as PLGA-PEG. Sodium cholate (SC) was optionally added to the aqueous phase in order to compare the two processes in the very same conditions. The different formulations characteristics such as hydrodynamic diameter (d_H), polydispersity index (PDI) and encapsulation efficiency of PFOB (η_{encaps}) are presented in Table 1.

The order of addition of each phase was investigated. It is shown that when the solvent is poured in the water phase, nanoparticles of around 120nm with high PDI values are obtained: 0.31 and 0.37 with and without SC respectively. The high polydispersity values can be explained by the very quick diffusion of the organic phase into the aqueous one followed by rapid and turbulent capsule formation, as already observed [33]. In addition, the PFOB encapsulation efficiency is high: η_{encaps} = 73 ± 2% and 70 ± 1% with and without SC respectively. Nevertheless, the nanoparticles recovery is low (48 and 41%), as seen by weighing freeze dried samples before and after filtration (0.45µm). Optical microscopy reveals the presence of microcapsules of 2-6µm. In the opposite way, adding the aqueous phase to the solvent leads to slightly larger but less polydisperse objects. In this case, suspensions are turbid which is surprising since suspensions of nanocapsules are usually very transparent as PFOB refractive index is 1.30 (25°C) close to the one of water [34]. Nanoparticles and nanocapsules are probably formed all together, which is also evidenced by the low encapsulation efficiencies: η_{encaps}= 30 ± 3% and 31 ± 2%, respectively with and without SC.

Influence of sodium cholate on nanocapsule characteristics was also determined. This surfactant seems to have a little influence on size and polydispersity of the objects, however it controls their morphology. In absence of SC, acorn morphologies, in which a hemisphere of liquid PFOB coexists with a hemisphere of solid PLGA-PEG, are observed by optical microscopy. Actually, PLGA-PEG is a poor stabilizer for the methylene chloride-water interface compared to sodium cholate. The interfacial tension is lowered from 28.2 mN/m to 17.5 mN/m in presence of 25 mg/mL copolymer, while it reaches 8.1mN/m, when the aqueous phase contains 1.5 w/v % of SC [13, 35].

To conclude, none of the studied nanoprecipitation conditions fulfils the requirements for the production of PLGA-PEG nanocapsules in terms of size (d_H~150nm), polydispersity (PDI<0.20) and PFOB encapsulation efficiency. Emulsion-evaporation conditions seem to be more satisfying, considering Table 2. With PLGA-PEG, the objects are around 120nm, have a low PDI (0.18) and very high encapsulation efficiency (85 ± 4%), suggesting that the majority of the objects corresponds to nanocapsules. When PLGA is used, capsules are almost of the same size d_H=130nm but are more polydisperse, PDI=0.24, and encapsulate a reduced quantity of PFOB: η_{encaps}=63 ± 7%. Independently of the polymer used, the encapsulation efficacy of PFOB is much higher as compared with other studies: Srinivas et al. only succeeded to encapsulate 8% of PFOB in PLGA using the very same

process [9]. This difference most probably arises from the use of PVA as surfactant instead of SC. The relevance to formulate PLGA-PEG by an emulsion-evaporation process is thus confirmed in order to produce PEGylated nanocapsules and will be used in the following of the article.

Morphology

PLGA and PLGA-PEG nanocapsules were observed by Scanning Electron Microscopy. Images show spherical objects with sizes in good agreement with the hydrodynamic diameter measured by dynamic light scattering (Figure 1). In addition, smooth surfaces are observed for both nanocapsules. For PLGA-PEG nanocapsules, this result contrasts with previous experiments showing that microcapsules obtained by emulsion-evaporation present spongy/porous surfaces [35]. The porous morphology was arising from the necessity to create surface to accommodate all PEG chains in the aqueous environment. Since nanocapsules possess a smooth surface, one can assume that the specific surface of nanocapsules is large enough for all PEG chains to be exposed to the aqueous environment.

Morphological analysis was completed by Transmission Electronic Microscopy imaging, which confirms that the core-shell structure is preserved with PLGA-PEG. The PFOB core appears in grey, whereas the polymeric shell seems darker. The intrinsic contrast between PFOB and PLGA-PEG has already been observed for PLGA nanocapsules. However, the shell of the PLGA-PEG nanocapsules appears more diffuse than the one for PLGA, considering previously published pictures [32]. The PEG chains are fully hydrated, lowering the contrast between the shell and water, leading to a blurry surface (Figure 1).

Nanocapsule purification

Sodium cholate, a bile salt is obviously tolerable by intestinal cells when given orally but is reported to destabilize cell membranes, and cause hemolysis in the blood at concentration of 1 to 20mM [36-37]. An intravenous administration of nanocapsules requires ensuring SC removal. PLGA and PLGA-PEG nanocapsule suspensions were purified by ultracentrifugation to remove SC. The concentration of SC in native suspension and supernatant were measured by UV-spectrophotometry in H_2SO_4 at 320nm (Table 3). In water, since SC has no chromophore, the molecule cannot be quantified by spectrophotometry. However, when dissolved in concentrated sulfuric acid solution, dehydration of the alcohol functions occurs, giving alkene functions. Thanks to the double bonds, quantification by spectrophotometry is made possible.

Sodium cholate was efficiently removed by this method since 99.45 ± 1% (PLGA-PEG) and 99.55 ± 1% (PLGA) of the initial amount in suspension, is recovered in the supernatant. The remaining SC,

[SC]≤0.15 mM, can be neglected. It is very close to the detection limit of UV spectrophotometry, around 10^{-4}M, 10 times lower than reported haemolytic dose [36-37].

After purification, PLGA-PEG nanocapsules preserve both their size and low polydispersity (Table 2). No aggregation occurs during the centrifugation, probably thanks to steric repulsions of PEG chains. After purification, PLGA-PEG nanocapsules zeta potential decreases from -15.6mV to -29.3mV, since surface charges are no longer screened by the concentrated sodium cholate. Indeed, when the same initial amount of SC is added to the purified formulation, the zeta potential recovers almost perfectly its initial value (ζ=-15.9 mV). For PLGA nanocapsules, size increases from 130.4 ± 3 nm to 175.1 ± 0.2 nm and the zeta potential becomes neutral (ζ=-0.02mV) due to the presence of residual PVA chains on nanocapsule surface, as already observed [3, 38]. Strong interaction by hydrogen bonding between PVA and PLGA are favoured during incubation.

Stability

PLGA copolymers are known for their biodegradability and biocompatibility. The degradation is characterized by random hydrolytic scission of the polyester backbone. The higher the glycolide content, the faster the degradation. For PLGA 50:50, final products: lactic and glycolic acids are detected from the first day in the medium [39]. In this case, *in vitro* degradation of PLGA-PEG nanocapsules was assessed by following the size and PFOB content variations in PBS buffer (pH=7.4) at 37°C (Figure 2). At the beginning of the study, nanocapsules are slightly bigger than reported in table 2, d_H=154 ± 2 nm. This increase in size can be explained by a higher swelling of the shell due to formation of carboxylic acid and hydroxyl groups among PLGA in PBS. Then the size remains almost constant for 120h. Small variations of the PFOB concentration occur during the first 48h. Between 48h and 120h, drop of the PFOB content and appearance of aggregates in the suspensions, evidence the disintegration of the nanocapsules. Considering the relative loss of PFOB, it can be estimated that only around 11% of nanocapsules are destroyed after 120h, the remaining ones preserve their sizes.

Nanocapsule PEGylation

To ascertain the presence of PEG moieties on PEGylated nanocapsule surface, XPS experiments were performed. The high resolution C1s region was recorded and peak fitted for the raw polymers PLGA and PLGA-PEG, as references and for nanoparticles of both types. Some of the parameters were set during peak fitting. First the binding energy positions of peaks were located according to the literature [38, 40]. Secondly, the intensities of ester and methine peaks were strained to be equal, since PLGA 50:50 comprises both functions in the same proportion [41]. PLGA spectra indicates 3 distinct peaks namely aliphatic carbon (C-C) at 285 eV, methine carbon (O=C-C*-O) at 287.0 eV and ester carbon (O=C-O) at 289.2 eV. Meanwhile 4 C1s peaks appear on the PLGA-PEG spectra, the

additional peak resulting from an ether group (C-O) at 286.2 eV, characteristic of PEG (Figure 3). The insertion of this fourth peak slightly shifts the peak binding energies of methine and ester carbons to higher energies, respectively 287.3 eV and 289.4 eV. We obtained excellent agreement between experimental and curve fit data for the raw PLGA-PEG polymer. For the PLGA-PEG nanoparticles, the half-height width of peaks is larger, enlightening the amorphous state of the polymeric shell. Table 4 summarizes atomic composition for the C1s peak fitting results. Considering the chemical formula of the used $PLGA_{346}$-PEG_{114}, the theoretical value of the ratio between atomic percentages of ether carbon and ether and ester carbons taken together, is 24.8%. The experimental value is 26.2%. The small difference may be explained by the rather high polymolecularity of the copolymer. This ratio is increased to 38.1% for the PLGA-PEG nanoparticles. Ether functions enrichment reveals that PEG chains are surface oriented in the case of nanoparticles [42]. This is probably occurring during the emulsion-evaporation process. As the PLGA-PEG reaches its solubility limit in methylene chloride, it migrates to the interface and exposes the hydrophilic PEG moieties toward the aqueous phase [35]. Assuming all PEG chains are present at nanocapsule surface, the available surface for each PEG chain, S^{PEG}, can be evaluated as follows:

$$S^{PEG} = \frac{m_{NC} S_{sp}^{NC}}{N_{PEG}} \qquad S_{sp}^{NC} = \frac{6}{d_H \rho}$$

where m_{NC} is the weight of nanocapsules obtained at the end of the process (m_{NC}=140mg), N_{PEG} is the total number of PEG chains in the final formulation, easily calculated from m_{NC} and η_{encaps}=85%, S_{sp}^{NC} is the specific surface area of nanocapsules estimated from d_H, the hydrodynamic diameter of nanocapsule (d_H=120nm) and ρ, the density of nanocapsule, measured by densimetry, ρ =1.5g/cm^3. Finally, one PEG chain occupies an area of around 5nm² at nanocapsule surface. This value is very close to 2nm², which is considered as the optimal surface to ensure minimal adsorption of opsonins [43].

Evaluation of complement activation

The complement system ensures the innate immune response, which consists in non-specific recognition of foreign bodies (i.e. opsonisation). Complement activation cascade is complex and consists in a chain of bio-chemical reactions [44-45]. One triggering factor is the binding and the conformational changes of the plasma protein C3. The native form is then cleaved into two fragments: C3a and C3b. 2D immunoelectrophoresis was used to compare the relative amount of these three species after incubation of PEGylated and plain nanocapsules in serum. The capacity of the different nanocapsules to trigger complement activation was evaluated. The influence of the surface area (A/ 1000 and B/ 2000cm²) was studied by changing the concentration of nanocapsules in

the incubated serum. The four gels obtained (Figure 4) show the presence of two peaks. The higher one, on the left side corresponds to the native C3 protein, while the large double peak on the right side reveals the activation of the protein with production of the two smaller fragments: C3a and C3b.

At low surface area (1000cm²), the two types of nanocapsules induce a similar and weak activation of the complement activation, evidenced on the electrophoregram by a larger C3 peak as compared with C3a and C3b. One obtains a CAF value of 19 ± 3% for PLGA and an even lower one for PLGA-PEG: CAF=14 ± 3%. Since the CAF difference is of the same order of magnitude as the experimental error, around 5%, the two types of nanocapsules cannot really be distinguished [31]. The residual PVA coating on PLGA nanocapsules might protect plasma protein adsorption by steric repulsion [46]. At higher surface area (2000cm²), the difference between PLGA and PLGA-PEG nanocapsules becomes clearer. On one hand, PLGA-PEG activation remains very low (CAF=11 ± 2%). On the other hand, for PLGA, the right peak increases noticeably and the activation is moderate (CAF value is 32 ± 2%).

Low activation of PEGylated nanocapsules, even at very high concentration ($S_{spé}$~2000 cm² C_{NC}= 66.7 mg/mL) is noticeable. From a complement activation point of view, PEG coverage is more efficient than PVA coating. The hydrophilic chains probably adopt a brush conformation and prevent serum protein adsorption more efficiently. Since the *in vitro* evaluation of complement activation is considered to be predictive of the *in vivo* fate of nanocapsules after intravenous administration [47]: PLGA-PEG nanocapsules should therefore be more stealth than PLGA ones.

In Vivo ^{19}F Magnetic Resonance Imaging

Kinetic study

In vivo ^{19}F MR imaging was performed in four mice after intravenous injection of PLGA and PLGA-PEG nanocapsules. After 4 hours, both types of nanocapsules are mainly accumulated in the spleen and liver (data not shown). Since the chosen MRI sequence does not allow any observation of the vascular compartment, the ^{19}F signal only arises from the immobilized nanocapsules in the tissues [11]. Liver and spleen uptake kinetics were studied in more details for the first 90 minutes after intravenous injection.

For the spleen, kinetic profiles for PLGA and PLGA-PEG nanocapsules do not follow any characteristic trend and interanimal variability is high (data not shown). This probably arises from the complex mechanism of spleen capture and the numerous functions of the organ (erythrocyte conditioning and maintenance, platelet storage, immune functions...) which can interfere with each other. In any case, after 90 minutes the fractions of nanocapsules accumulated are 5.3±0.2% and 5.7±1.7% for

PLGA and PLGA-PEG nanocapsules, respectively. These values are very similar for both types of nanocapsules and in agreement with those found for poloxamer coated polystyrene or PHDCA-PEG nanoparticles of the same size [25, 48]. Splenic uptake is often compared to a filtering or a sieving process, particularly effective to remove poorly opsonized antigens, therefore it does not depend on the nanoparticles surface properties [49].

For the liver, the kinetic profiles present less interanimal variability. The fraction of nanocapsules accumulated in the liver increases continuously as a function of time until it reaches a plateau value of 12.5% of injected dose for PLGA capsules. For PLGA-PEG capsules, accumulation increases until 16.1% of the injected dose after 90 minutes but the plateau is probably not reached yet (Figure 5). A two-compartment model was chosen for experimental data fitting, meaning that nanocapsules are transferred from the bloodstream to the liver compartment. The time dependency of the nanocapsule concentration (via PFOB concentration) in the organ is given by the following formula:

$$C_{PFOB}(t) = C_0^{liver}[1 - \exp(-k_{liver}t)]$$

The fitted values of C_0^{liver} and k^{liver} are reported in table 5. R values are higher than 0.94 for the 4 mice, confirming the accuracy of the fits.

The half-life absorption constant k^{liver} is calculated as: $t_{1/2} = \ln(2)/k^{liver}$. PLGA nanocapsules fit yields $t_{1/2}^{PLGA}$=13.6 min whereas PEGylated nanocapsules circulate longer with $t_{1/2}^{PLGA\text{-}PEG}$=23.9 min. These results confirm the efficacy of our strategy for stealthiness. Accumulation occurs in approximately the same time for PLGA nanocapsules as compared to polysaccharide-coated nanoparticles ($t_{1/2}$=14min) [50] or PEGylated PFOB emulsions ($t_{1/2}$=11.7min) [11]. The rate of liver accumulation is divided by 1.8 for PLGA-PEG nanocapsules. For PLGA, the liver uptake starts to saturate after one hour whereas nanocapsules keep accumulating after 90 minutes for PLGA-PEG. Most probably PLGA-PEG nanocapsules remain in the blood circulation after 90 minutes. These results agreed with the complement activation results.

In vivo tumor imaging

CT26 cells are highly tumorigenic at doses ranging from 10^5 to $4*10^6$ cells. Subcutaneously inoculated, they produce well vascularized tumors. Dense angiogenic network was evidenced from day 7 after inoculation [51-52]. *In vivo* ^{19}F MR imaging was achieved in five mice 7 hours after intravenous injection of PLGA (2 mice) and PLGA-PEG (3 mice) nanocapsules. For PLGA capsules, after 7 hours the fractions of injected dose in the spleen (1.75 ± 0.2%) and liver (9.70 ± 2.5%) are lower than values obtained 90 minutes after injection. Nanocapsules accumulated in these organs are progressively eliminated and the circulating fraction probably starts to degrade. On the contrary, for

PLGA-PEG nanocapsules, fractions found in the organs 7 hours after injection are higher than those found 90 minutes after injection: 6.8 ± 1.9% in the spleen and 18.9 ± 1.5% in the liver. Nanocapsule elimination from the liver and spleen is compensated by their continuous uptake (Figure 6).

Tumor accumulation confirms these results. For PLGA nanocapsules, the ^{19}F signal in the tumor does not exceed the background noise arising from the rest of the viscera. The detection limit was evaluated to be C_{PFOB}=0.04mM for 35 minutes of acquisition. For PLGA-PEG nanocapsules the intensity is weak in the tumor but the concentration of PFOB could be quantified: C_{PFOB}= 0.19 ± 0.02 mM (Figure 7), corresponding to about 1% of the injected dose (n=2), of the same order of what is usually observed [53-54]. Altogether, these results prove the efficacy of PEGylation to increase the residence time of nanocapsules in the blood stream, allowing them to reach tumors by EPR effect.

Conclusion

Encapsulation of PFOB with PEGylated nanocapsules of PLGA-PEG has been optimized by the solvent emulsion-evaporation method, leading to nanocapsules of about 120nm with a high yield of encapsulation of PFOB around 80%. The PEG coverage seems rather dense allowing low complement activation *in vitro*. ^{19}F-MRI was used to follow the liver and spleen accumulation and revealed that PEGylated nanocapsules were circulating longer than their plain counterparts ($t_{1/2}^{PLGA}$=13.6min and $t_{1/2}^{PLGA\text{-}PEG}$=23.9min). This enhanced circulation time was further confirmed by the ability to detect implanted tumors 7 hours after PEGylated nanocapsule intravenous injection. These PEGylated nanocapsules appear promising for detecting tumors using the EPR effect using ^{19}F-MRI. Future studies will focus on nanocapsule accumulation as a function of tumor growth stage and the imaging time post-injection.

Acknowledgements

Authors acknowledge financial support from Fondation de l'Avenir (ET9-545). Authors would like to thank M-F Trichet for access to the SEM facility (ICMPE, Thiais, France), D Jaillard for TEM experiments, E. Morvan for her help with ^{19}F NMR spectroscopy, and N. Mignet and J. Seguin for providing fruitful advice for tumor growth. Our laboratory is a member of the Laboratory of Excellence LERMIT supported by a grant from ANR (ANR-10-LABX-33).

Tables and Figures

	% SC (w /v)	d_H (nm)	PDI	η_{encaps} (%)
Solvent in water	0	122 ± 3	0.37	70 ± 1
	1.5	120 ± 2	0.31	73 ± 2
Water in solvent	0	145 ± 0.1	0.16	31 ± 2
	1.5	178	0.19	30 ± 3

Table 1 : Characteristics of nanocapsules obtained by nanoprecipitation (n=2).

		d_H (nm)	PDI	ζ (mV)	η_{encaps} (%)
PLGA-PEG	After preparation	121 ± 2	0.18	-16±6	85 ± 4
	After purification	123 ± 4	0.16	-29±11	-
PLGA	After preparation	130 ± 3	0.24	-70±19	63 ± 7
	After purification	175 ± 0.2	0.18	0±5	-

Table 2 : Characteristics of nanocapsules obtained by the emulsion evaporation process and after the purification step (n=3).

		[SC] (mM)
Suspension	PLGA-PEG	29.01 ± 1.28
	PLGA	28.94 ± 0.28
Supernatant	PLGA-PEG	29.15 ± 1.02
	PLGA	28.80 ± 0.12

Table 3 : SC Concentration, calculated from the measured absorbance at 320nm, in the just prepared suspensions of PLGA and PLGA-PEG nanocapsules and in their supernatants collected after ultracentrifugation. Data correspond to mean ±SD, n=3.

	Atomic % of C1s, high resolution			
	Aliphatic C-C	Ether C-O	Methine O=C-C*-O	Ester O=C-O
PLGA	16.60 (285 eV)	0	41.70 (287.0 eV)	41.70 (289.2 eV)
PLGA NPs	19.75 (285 eV)	0	40.42 (287.0 eV)	39.83 (289.2 eV)
PLGA-PEG	29.69 (285 eV)	10.54 (286.2 eV)	30.03 (287.3 eV)	29.73 (289.4 eV)
PLGA-PEG NPs	12.55 (285 eV)	20.61 (286.2 eV)	33.42 (287.3 eV)	33.42 (289.4 eV)

Table 4 : Relative atomic percentages from the area under the curves of fitted peaks, whose positions in binding energy appear in the brackets.

	PLGA	PLGA-PEG
C_0^{liver} (Fraction of injected dose)	12.4 ± 2.2%	16.1 ± 3.1%
k^{liver} (min^{-1})	0.051 ± 0.008	0.029 ± 0.0008

Table 5 : Fitted kinetic parameters for PLGA and PLGA-PEG nanocapsules in the liver (n=2).

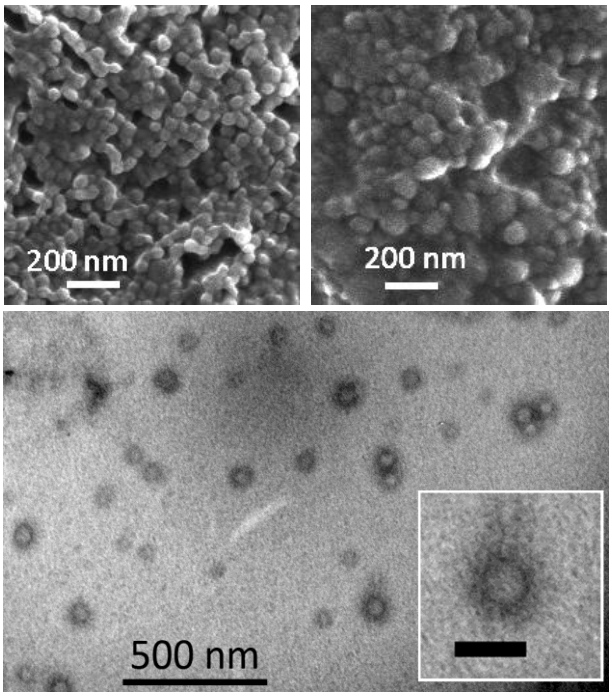

Figure 1: Top: SEM images of PLGA (left) and PLGA-PEG (right) nanocapsules Bottom: TEM images of PLGA-PEG nanocapsules with intrinsic negative contrast of the polymer. The insert is a zoom on one capsule (scale bar 100nm). The PFOB core is surrounded by a cloudy shell.

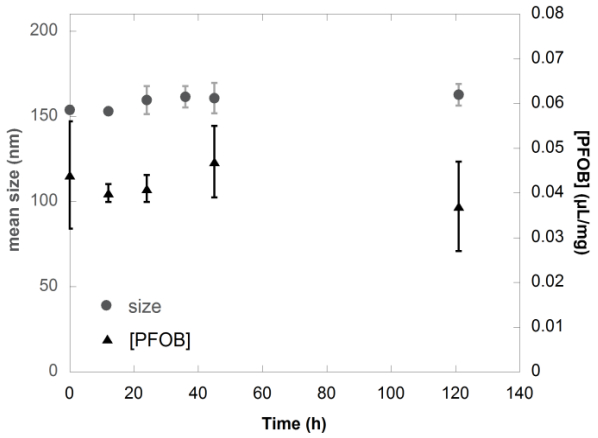

Figure **2**: Evolution of size and PFOB concentration during the incubation of PLGA-PEG nanocapsules in PBS buffer at 37°C.

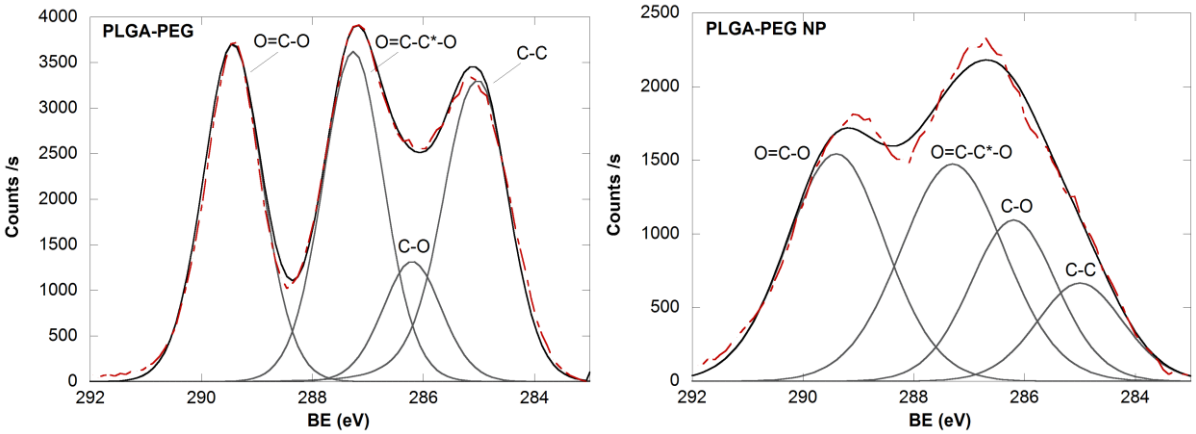

Figure 3 : High resolution XPS spectra of C1s region for the raw PLGA-PEG polymer (left) and the corresponding nanoparticles (right). Red dashed line corresponds to experimental data whereas black full lines represent the fits.

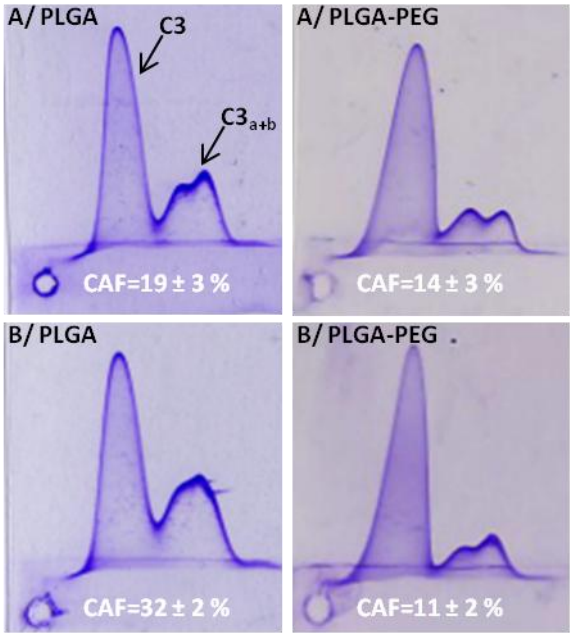

Figure 4 : Profiles of complement activation for PLGA and PLGA-PEG nanocapsules as revealed by 2D electrophoresis of C3 antigen and their corresponding CAF values. Concentrations of nanocapsules were chosen to obtain a surface area of A/ 1000 cm^2 and B/ 2000 cm^2. CAF=$C3_{a+b}$/(C3+$C3_{a+b}$).

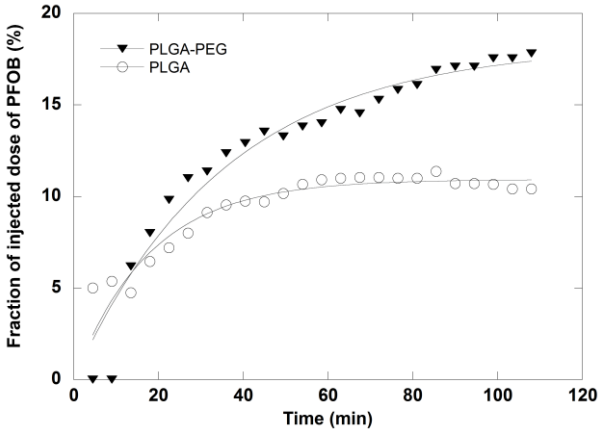

Figure 5 : Evolution of the PFOB concentration in the liver, as measured by ^{19}F MRI during the first 90 minutes following the IV administration of PLGA or PLGA-PEG nanocapsules.

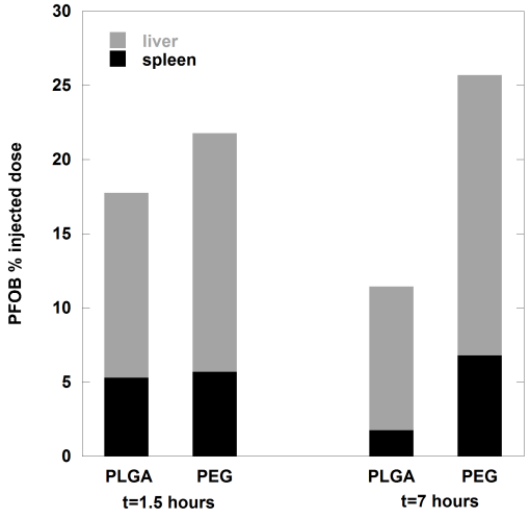

Figure 6: Cumulative PFOB accumulation in the liver and spleen 1.5 hours (left) and 7 hours (right) after nanocapsule injection.

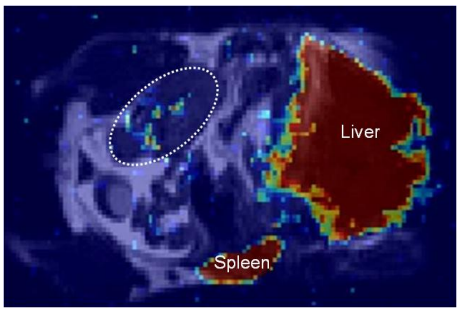

Figure 7 : ^{19}F MR image superimposed with anatomical ^{1}H MR image of a tail-head longitudinal cross section of a mouse 7 hours after intravenous injection of PLGA-PEG nanocapsules for a tumor of 720mm^3 (white dotted circles).